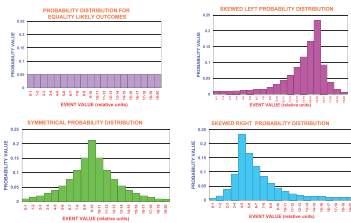


Applications of Statistics to Medicine and Medical Physics

Edward L. Nickoloff



MEDICAL PHYSICS PUBLISHING

Here is a sample chapter
from this book.

This sample chapter is copyrighted and made available for personal use only. No part of this chapter may be reproduced or distributed in any form or by any means without the prior written permission of Medical Physics Publishing.

Applications of Statistics to Medicine and Medical Physics

Applications of Statistics to Medicine and Medical Physics

Edward L. Nickoloff, D.Sc.

FACR, FAAPM, and FACMP

Professor of Radiology

Columbia University and

New York-Presbyterian Hospital

New York, New York

MEDICAL PHYSICS PUBLISHING

Madison, Wisconsin

Copyright © 2011 by Edward L. Nickoloff

All rights reserved. No part of this publication may be reproduced or distributed in any form or by any means without written permission from the publisher.

15 14 13 12 11 1 2 3 4 5 6

Library of Congress Control Number: 2011924799

ISBN 13: 978-1-930524-51-4 hardcover

ISBN 13: 978-1-980524-71-2 2014 eBook edition

Medical Physics Publishing
4513 Vernon Boulevard
Madison, WI 53705-4964
Phone: 1-800-442-5778, 608-262-4021
Fax: 608-265-2121
Email: mpp@medicalphysics.org
Web: www.medicalphysics.org

Notice: Information in this book is provided for instructional use only. The author and publisher have taken care that the information and recommendations contained herein are accurate and compatible with the standards generally accepted at the time of publication. Nevertheless, it is difficult to ensure that all the information given is entirely accurate for all circumstances. The author and publisher cannot assume responsibility for the validity of all materials or for any damage or harm incurred as a result of the use of this information.

Printed in the United States of America on acid-free paper

Dedication

This book is dedicated to my son, Edward Jr., and my daughter, Andrea Lee.

They have both taught me many life lessons, such as perseverance of goals despite numerous obstacles and adversities in the path toward those goals. The future will depend upon the character, motivation, capabilities, and efforts of our young people.

I believe that the future will be marvelous because of the exuberance and determination of the next generation.

Contents

<i>Preface</i>	xiii
----------------------	------

I Fundamental Concepts and Their Applications

1.1	Permutations.....	1
1.2	Combinations.....	2
1.3	Frequency Distribution.....	4
1.4	Median, Mode, and Mean.....	6
1.5	Quartiles	7
1.6	Cumulative Frequency Distribution	7
	Useful References.....	8
	Practice Exercises.....	9

2 Probability Distribution

2.1	Introduction to Characteristics of Probability Distributions	13
2.2	Binomial Probability Distribution	18
	2.2.1 Fundamentals.....	18
	2.2.2 Application A.....	22
	2.2.3 Application B.....	23
	2.2.4 Application C.....	24

viii ■ Contents

2.3	Poisson Probability Distribution	25
	2.3.1 Fundamentals.....	25
	2.3.2 Applications.....	27
2.4	Normal Probability Distribution.....	29
	2.4.1 Fundamentals.....	29
	2.4.2 Application A.....	31
	2.4.3 Application B.....	32
2.5	Log Normal Probability Distribution	34
	2.5.1 Fundamentals.....	34
	2.5.2 Application	37
2.6	Error Function	38
	2.6.1 Basics.....	38
	2.6.2 Application	43
	Useful References.....	45
	Practice Exercises.....	46

3 More Details about the Normal Probability Distribution

3.1	The Mean.....	49
3.2	The Standard Deviation.....	50
3.3	Statistical Sampling.....	51
3.4	Applications of Mean and Standard Deviation.....	52
	3.4.1 Estimation of the Standard Deviation	52
	3.4.2 Relative Standard Deviation.....	54
3.5	Standard Deviation for Addition and Subtraction Operations.....	55
3.6	Standard Deviation for Multiplying or Dividing Operations	56
3.7	Standard Error of the Mean	59
3.8	The Cumulative Normal Probability Distribution.....	60
3.9	Approximation to the Cumulative Normal Probability Distribution.....	62
3.10	Confidence Intervals.....	64
3.11	Logit Transforms	66
3.12	Applications.....	70
	Useful References.....	72
	Practice Exercises.....	73

4 Separation of Two Statistical Populations

4.1	Variation of Sample Mean	75
4.2	Separation of Two Different Normal Population Distributions.....	76
4.3	The Decision Matrix.....	77

4.4	Receiver Operating Characteristic (ROC) Graphs	82
4.5	Student's T-Test	84
4.6	Required Sample Size	86
4.7	Chauvenet's Criterion.....	87
4.8	Chi-Square Test for "Goodness of Fit"	88
4.9	Applications.....	90
	Useful References.....	93
	Practice Exercises.....	94

5 Bayes' Theorem

5.1	Basics.....	97
5.2	Patient Population Characteristics.....	99
5.3	Applications.....	103
	Useful References.....	108
	Practice Exercises.....	109

6 Graphical Fits to Measured Data

6.1	Basics of Linear Regression	113
6.2	Inverse Matrix Approach to Linear Regression	119
6.3	Polynomial Fit to Data	123
6.4	Exponential Functions.....	127
6.5	Logarithmic Functions	131
6.6	Power Functions.....	132
6.7	Standard Error of the Estimate (SE).....	135
	Useful References.....	141
	Practice Exercises.....	142

7 Correlation Function

7.1	Linear Correlation Coefficient	149
7.2	Alternate Form for Linear Correlation Coefficient	151
7.3	How Significant Is the R^2 Value?	153
7.4	Terminology for Correlation.....	155
7.5	Correlation for Nonlinear Functions	157
	Useful References.....	158
	Practice Exercises.....	159

8 Fractals and Their Applications

8.1	Basic Concepts	163
8.2	Examples of Fractals in Nature	169
8.3	Applications of Fractals to Human Anatomy	175
8.4	Mandelbrot Sets.....	170
	Useful References.....	183
	Practice Exercises.....	183

9 Monte Carlo Methods

9.1	Random Numbers.....	187
9.2	Random Walk	190
9.3	Illustrations of Monte Carlo Process	192
	9.3.1 Application Using First Monte Carlo Example.....	196
	9.3.2 Application Using a Second Monte Carlo Example.....	198
9.4	Monte Carlo Analysis of X-Ray Photon Interactions.....	203
	Useful References.....	211
	Practice Exercises.....	212

10 Application of Statistics to Image Quality Measurements

10.1	Signal-to-Noise Ratio (SNR).....	215
10.2	Contrast-to-Noise Ratio (CNR).....	217
10.3	Contrast-Detail Diagrams.....	220
10.4	Detective Quantum Efficiency (DQE)	225
10.5	Noise Equivalent Quanta (NEQ).....	227
10.6	Digital Subtraction Angiography (DSA).....	227
	Useful References.....	234
	Practice Exercises.....	235

11 Misuse of Statistics

11.1	Introduction	237
11.2	Categories for Misuse of Statistics	242
	11.2.1 Sampling Error	243
	11.2.2 Influence of Bayes' Theorem.....	244
	11.2.3 Spurious Correlations	244
	11.2.4 Discarding Unfavorable Data	244

11.2.5 Mining Data.....	245
11.2.6 Ambiguous Evaluations.....	245
11.2.7 Systematic Errors.....	245
11.2.8 Verbal Context.....	246
11.3 Summary.....	246
Useful References.....	247
Appendix A: Normal Probability Distribution Tables.....	249
Appendix B: Two-Tailed Cumulative Normal Probability About the Mean Value Table.....	255
Appendix C: Lower One-Tailed Cumulative Normal Probability from $-\infty$ to X Table.....	259
Appendix D: Student's T-Test Value for Various Degrees of Freedom Table.....	265
Appendix E: Significance of the Correlation "R" Value Table.....	269
Index.....	275
About the Author.....	283

Preface

The motivation for writing this book had two specific goals. First, graduates students pursuing an advanced degree in medical physics are required to take a course in statistics; this book has many practical medical physics problems, which would make it ideal for this course. Although there are a number of statistic books available, there are no books that present statistics in a context that has applications important to medical physics and medicine. Second, most medical physicists are familiar with the very basics of statistical analysis such as mean and standard deviation; however, their ability to analyze data and to design statistically valid experiments may be limited. This book could serve as a key resource on statistical analysis for senior medical physicists or clinical researchers.

There are 11 chapters in the book, beginning with very basic topics like Binomial, Poisson, and Normal probability distributions and gradually progressing to more advanced topics such as log normal probability distributions, error functions, inverse matrix analysis, and logit transforms, which can be used for analyzing adverse effects of medications or contrast agents and to linearize film-screen characteristic curves. Clinical medical physicists and researchers must be able to analyze measured data; they must be able to determine whether two groups of data are statistically different using Student T-tests, Z-tests, Chi Square Goodness-of-Fit tests, as well as other tests. Chauvent's Criteria is used to determine whether to discard "bad" measurements. Information is provided about the usage of a decision matrix, accuracy, positive/negative predictive values, and receiver operating

characteristic (ROC) curves. Chapter 5 on Bayes' Theorem describes the influence of patient populations upon experimental results. Chapters 6 and 7 discuss, respectively, graphical data analysis, utilizing both linear and nonlinear functions, and correlation and the necessary design population and correlation coefficient (R value) for experimental studies. Two chapters introduce the usage of fractals (chapter 8) and Monte Carlo methods in medicine (chapter 9). The most important chapter, chapter 10, uses simple statistical methods to derive image analysis concepts like the signal-to-noise ratio (SNR), contrast-detail diagrams, detective quantum efficiency (DQE), and digital subtraction angiography (DSA). The last chapter discusses misuse of statistics, covering topics such as spurious correlations, influence of Bayes' Theorem, systematic errors, improperly discarding unfavorable data and other similar issues.

This book would make a valuable addition to any library due to the wide range of statistical topics and the many practical applications which are provided throughout the text. While learning statistics, medical physics graduate students would benefit from a book which addresses practical clinical topics rather than abstract statistical analysis, which is the approach of many other books on statistics.

Fractals and Their Applications

8.1 BASIC CONCEPTS

Fractals are obtained by using a process whereby self-similar structures are obtained from an object by adjusting the size of the object (either enlarging or minifying) by a specified magnification factor (R). Then, these self-similar objects are used to replace the original object or they are added to the original figure at some particular location by a rule. The process is then repeated many times. To illustrate this process, consider a straight line that is continuously reduced by half and used to replace the original line (illustration 8.1).

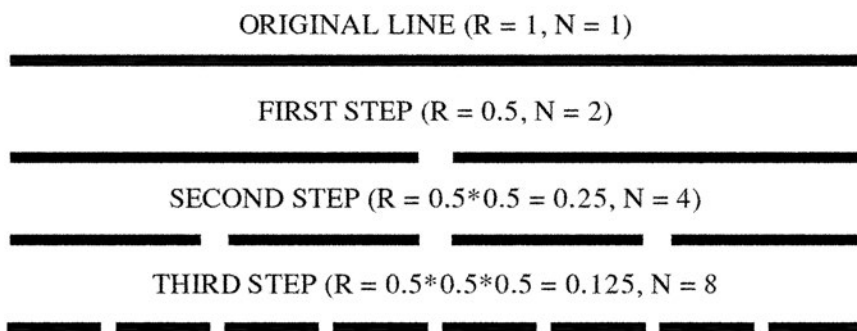


Illustration 8.1

As the minification increases, the original line segment is replaced by a greater number of smaller line segments. The number of segments is designated “N”. The number of line segments (N) can be given by the equation that relates the original line length (L) and the magnification factor (R):

$$N = [L/R]^D. \quad (8.1)$$

By taking a logarithm of both sides of the equation and rearranging the terms, equation (8.2) is obtained:

$$D = \frac{\text{Log}(N)}{\text{Log}(L/R)}. \quad (8.2)$$

The symbol “D” is called the *fractal dimension*. To illustrate this calculation, the fractal dimension (D) will be calculated for the third step shown in illustration 8.1. In this case, N = 8, R = 0.125, and L = 1.0.

$$D = \frac{\text{Log}(8.0)}{\text{Log}(1.0/0.125)} = \frac{\text{Log}(8.0)}{\text{Log}(8.0)} = 1.0 \quad (8.3)$$

Since this example deals with straight lines, it is not surprising that the fractal dimension is equal to one. Straight lines are one-dimensional objects in space.

Next, consider a square (see illustration 8.2). Again, envision the effect of using a magnification factor (R) equal to 0.5.

In this case, the original square is divided into four smaller squares. The fractal dimension in this case is:

$$D = \frac{\text{Log}(4.0)}{\text{Log}(1.0/0.5)} = \frac{\text{Log}(4.0)}{\text{Log}(2.0)} = 2.0. \quad (8.4)$$

Again, the fractal dimension of 2.0 is consistent with the fact that a square is a two-dimensional object.

Now, let us consider a cube that is replaced with cubes that are one-third the original size (see illustration 8.3). The magnification factor (R) would be 1/3.

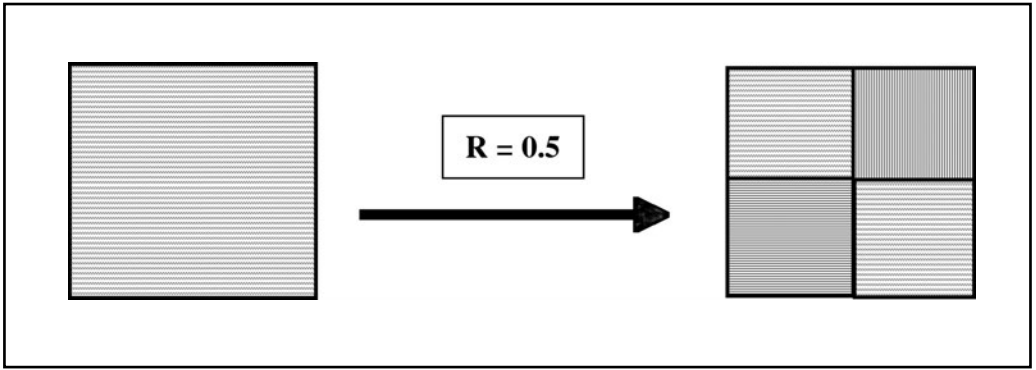


Illustration 8.2

In this case, the number of self-replicated pieces (N) is 27, or the original cube is replaced by 27 smaller cubes that are similar to the original. The fractal dimension for the new cube would be given by the expression below:

$$D = \frac{\text{Log}(27.0)}{\text{Log}(1.0/0.333)} = \frac{\text{Log}(27.0)}{\text{Log}(3.0)} = 3.0. \quad (8.5)$$

Since the cube is a three-dimensional object, it is again expected that the fractal dimension would also be 3.0.

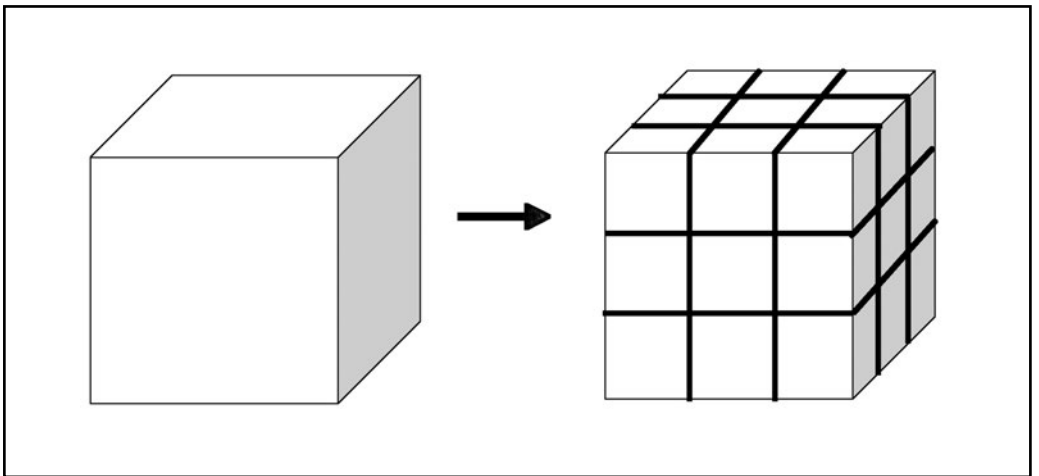


Illustration 8.3

However, there are objects for which the fractal dimensions are not whole numbers. One example is the Sierpinski triangle. The first step is to start with an equilateral, shaded triangle. A rule for the formation of subsequent Sierpinski triangles is to make inverted triangles of 0.5 the previous height and 0.5 the previous width. These inverted triangles are placed internally in each shaded triangle and are subtracted from the previous shaded triangles. This is illustrated in the figures in illustration 8.4.

In the second step, the original triangle becomes three smaller shaded triangles by subtracting a half-width and half-height triangle, which is placed inverted into the original triangle. In the third step, three smaller triangles are subtracted from the shaded triangles in step two. The remaining area equals nine shaded triangles. For this series of triangles, the fractal dimensions in both step 2 and step 3 are shown in equation (8.6).

$$D = \frac{\text{Log}(3.0)}{\text{Log}(1.0/0.5)} = \frac{\text{Log}(3.0)}{\text{Log}(2.0)} = 1.585 \quad (8.6)$$

$$D = \frac{\text{Log}(9.0)}{\text{Log}(1.0/0.25)} = \frac{\text{Log}(9.0)}{\text{Log}(4.0)} = 1.585$$

This fractal dimension is not a whole number. It has a dimension between one and two, and its numerical value is related to the complexity of the structures that are formed by following the fractal rule.

Another example also begins with a triangle (see illustration 8.5). The replication rule for self-similar objects is to divide each line segment into three parts. Then the middle line segment is removed and replaced by two line segments equal in length to the segment that is removed; these replacement line segments join in a point that looks like an added triangle. The process can continue indefinitely forming what looks like a (Koch) snowflake.

For the second step, the line segments are divided into three equal segments, or $R = 0.333$. The number of line segments increases from 3 line segments in the original triangle to 12; so N is equal to 12 divided by 3. For the third step, the line segments are divided into three again; R is equal to $(1/3)$ multiplied by $(1/3)$, or 0.111. The number of line segments increases to 48; so N is equal to 48 divided by 3, or 16.

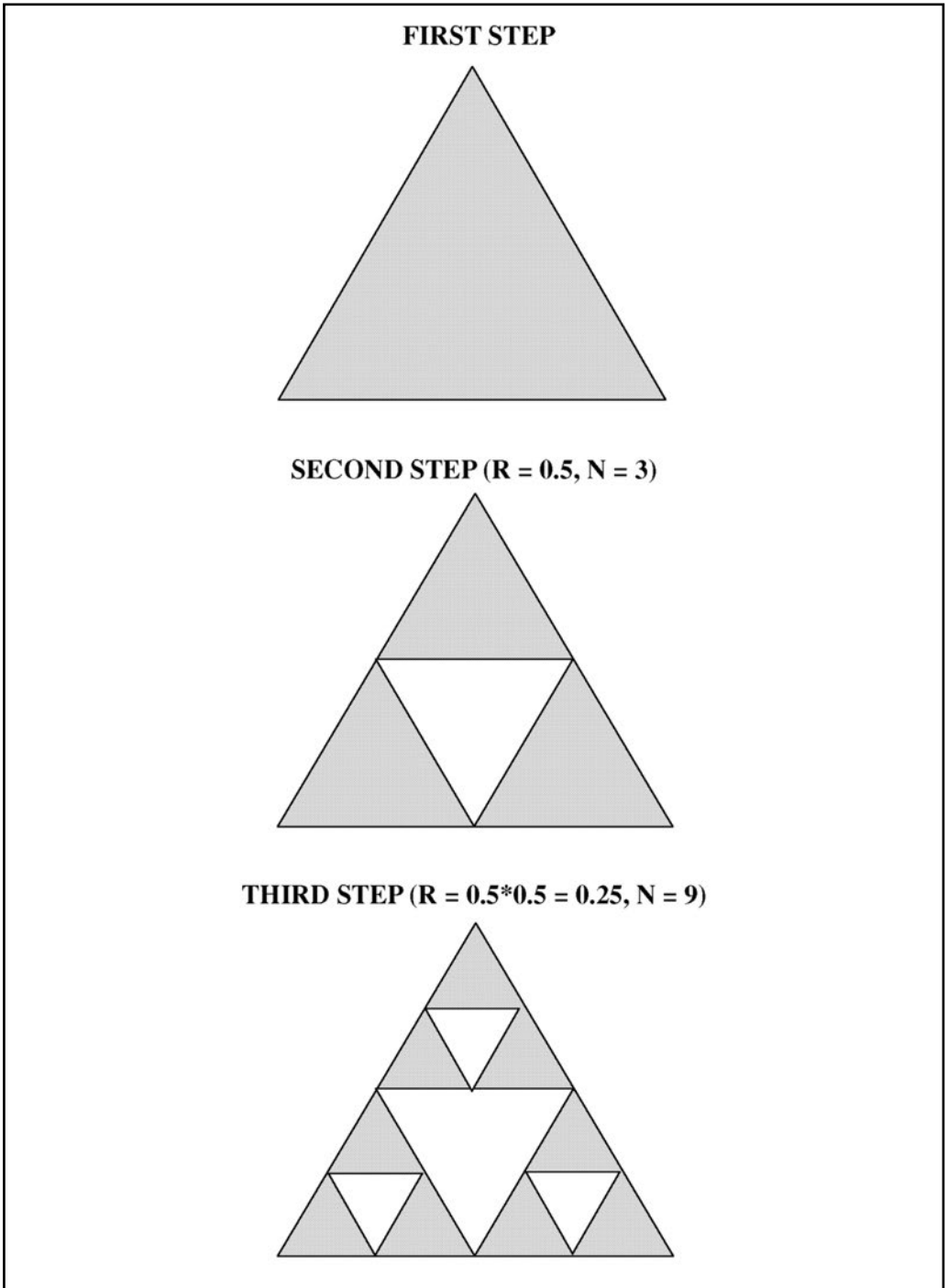


Illustration 8.4

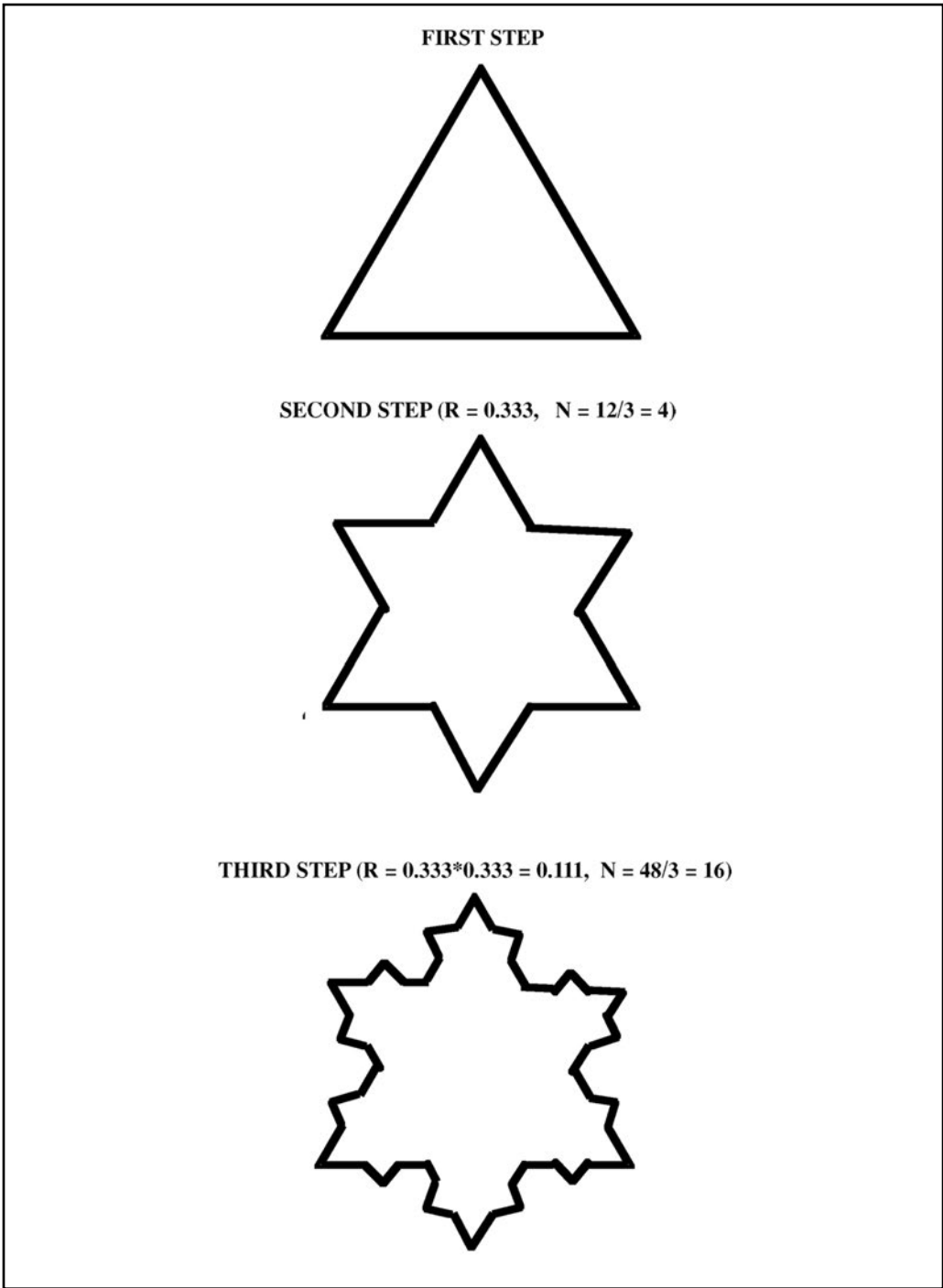


Illustration 8.5

For these series of figures, the fractal dimension is given below.

$$D = \frac{\text{Log}(4.0)}{\text{Log}(1.0/0.333)} = \frac{\text{Log}(4.0)}{\text{Log}(3.0)} = 1.262$$

$$D = \frac{\text{Log}(16.0)}{\text{Log}(1.0/0.111)} = \frac{\text{Log}(16.0)}{\text{Log}(9.0)} = 1.262 \quad (8.7)$$

Again, for this fractal figure, the fractal dimension is not a whole number that relates to the complexity of the design pattern. Although line segments were the parameter evaluated for these fractal objects, the fractal dimension is greater than 1.0, which is the normal value for a linear or line segment object.

There are many examples in nature for which the fractal dimension can be computed, and these structures have different fractal dimensions than regular geometric objects. The numerical value provides an index to the complexity of the object. For example, a tree consists of many repeated branches of its limbs, which could be analyzed by fractals.

8.2 EXAMPLES OF FRACTALS IN NATURE

Is there any practical application for these fractal concepts? Many objects in nature and in medicine cannot be described by some simple combination of rectangles, circles, cylinders, and spheres. The borders of real objects such as trees, coastal shorelines, clouds, and many other objects in nature are ragged and exhibit characteristics of fractal patterns when examined closely. Similarly, blood vessels in the human body, bronchi in the lungs, the EEG electrical signals, and portions of the human central nervous system might be modeled by fractal patterns.

The published literature contains examples where fractals have been utilized to evaluate the complexity of the coastlines of various countries. To illustrate this usage of fractals, we will examine the Florida coastline. The results depend upon the scale used to examine the shore. On a large scale, the shoreline may appear to be relatively smooth; however, by using a smaller unit of measurement, the complex nature of the coastline is better revealed. Illustration 8.6 shows a portion of the Florida coastline. The west coastline of Florida on the figure is measured with different scale factors.

By comparison to a single length measurement, the next smallest scale has an R equal to 0.235 and N equal to 6. The smallest measurement scale shown has an R value equal to 0.0353, and N equal to 41. In other words, the smallest scale of length shown fits 41 lines along the coastline whereas the medium scale fits only 6 lines along the same coastline. As the scale used to measure the coastline of Florida becomes smaller, more complexity in the variation of the shoreline is revealed. To evaluate this aspect of the coast, the fractal dimension is calculated for the medium and small scales shown on the map of Florida. For the medium scale measurement of the West Florida coast, the fractal dimension is shown by equation (8.8).

$$D = \frac{\text{Log}(N)}{\text{Log}(L/R)} = \frac{\text{Log}(6)}{\text{Log}(1.0/0.235)} = \frac{\text{Log}(6)}{\text{Log}(4.255)} \quad (8.8)$$

$$D = 1.237$$

For the smallest scale shown that is used to measure the length of the coastline, the fractal dimension is even smaller; a smaller fractal dimension indicates a smoother coastline.

$$D = \frac{\text{Log}(N)}{\text{Log}(L/R)} = \frac{\text{Log}(41)}{\text{Log}(1.0/0.0353)} = \frac{\text{Log}(41)}{\text{Log}(28.33)} \quad (8.9)$$

$$D = 1.111$$

The data for different size scales can be plotted in a graph with the abscissa “Log (L/R)” and the ordinate “Log (N)”, shown in illustration 8.7.

For this graph, the slope of the line is the estimated fractal dimension, D. The analysis of most coastlines in the published literature provides values between 1.02 for South Africa up to a value of 1.52 for the south coast of Norway. By comparison, the Florida west coastline is relatively smooth with a low fractal dimension. The fractal dimension is a useful parameter for the relative comparison of the ruggedness of the various coastlines.

Another application of fractals in nature is the analysis of branching structures such as trees and rivers. Trees generally bifurcate many times to produce their shape. With each change in the diameter of the branches (the scale factor), smaller and smaller branches are produced. However, a real tree is more complicated because it exists in three dimensions. The small branches can be at various angles to the main branches; and the

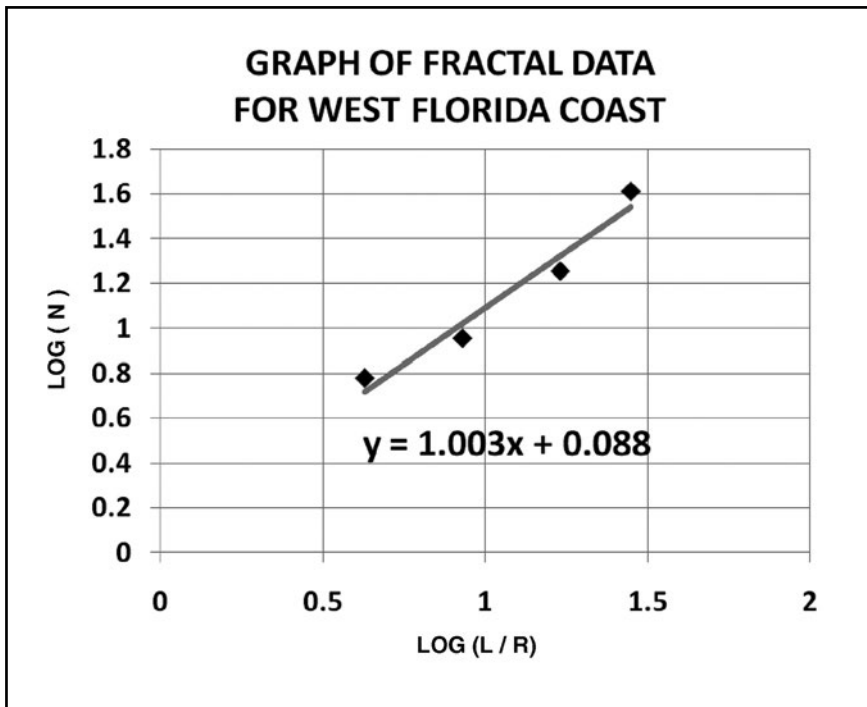


Illustration 8.7

smaller branches can be rotated at various angles around the main branch. Moreover, the branching is not always regular; there can be branches growing at anomalous locations. Illustration 8.8 demonstrates the process of branching in a real tree. There are many different species of trees, and each kind of tree may have its own branching pattern. Regardless, because of the self-replication of a generalized pattern, the branching of tree limbs can be modeled by fractals, and it can be characterized by a specific fractal dimension.

Three identical pictures are shown. On each picture, a grid is superimposed with different size blocks on the grid. The size of the blocks of the various grids is related to the R factor of fractals. For each grid, the number of blocks that contain a tree branch is counted; this number of blocks with objects inside is related to the N value of the fractals. The “Log (N)” is plotted as a function of the “Log (R)”. The slope is the fractal dimension, D. This method is called the *box counting* method of fractal analysis.

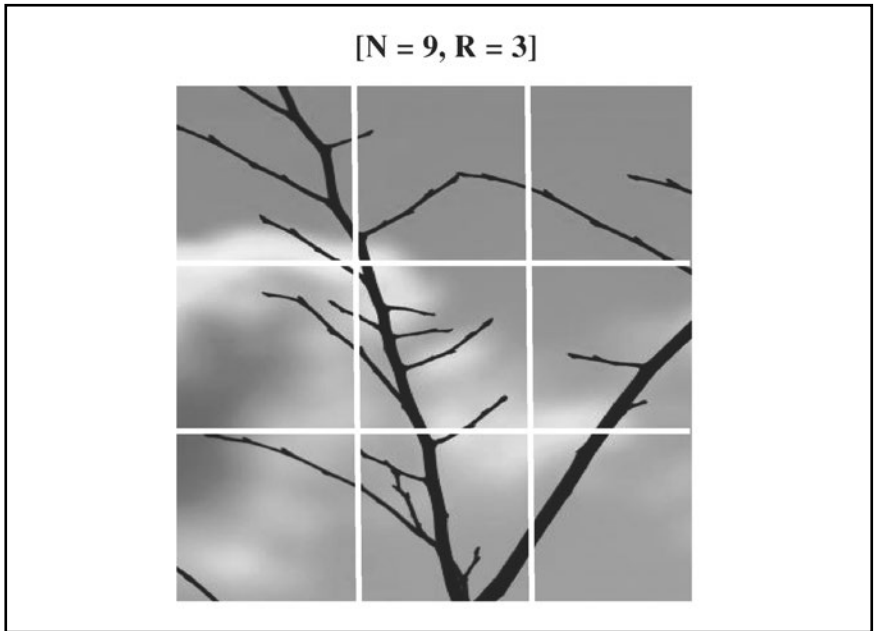


Illustration 8.8a

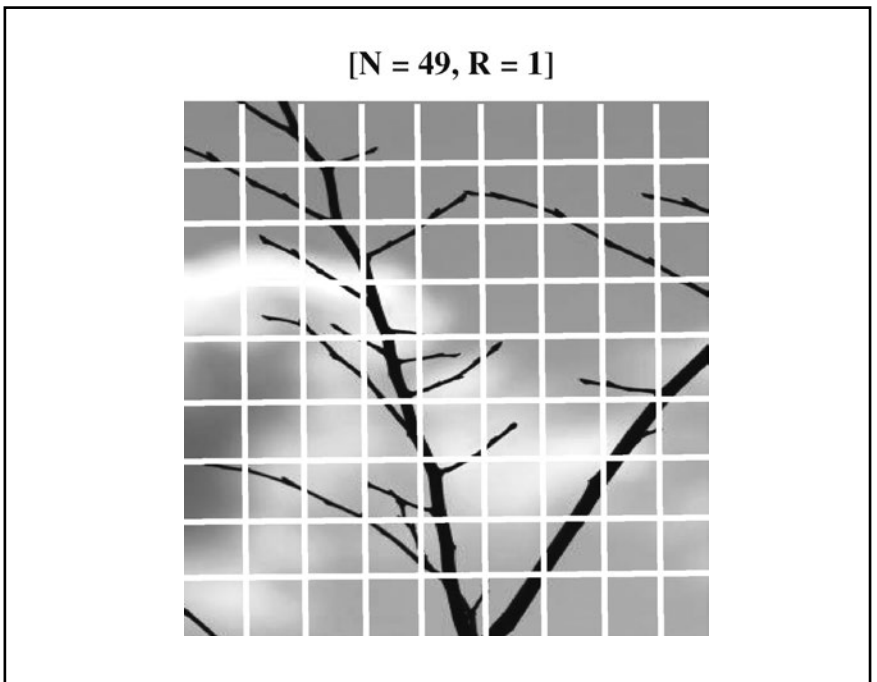


Illustration 8.8b

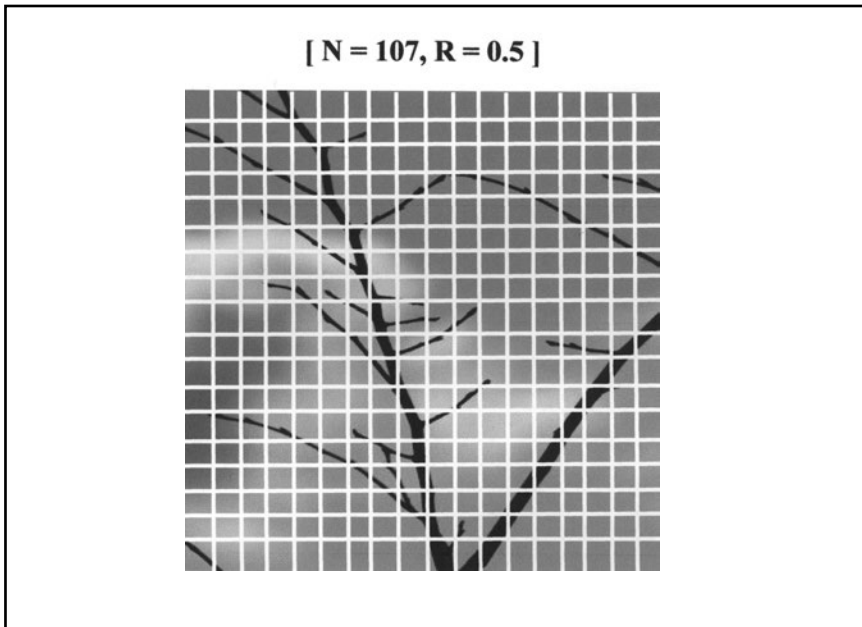


Illustration 8.8c

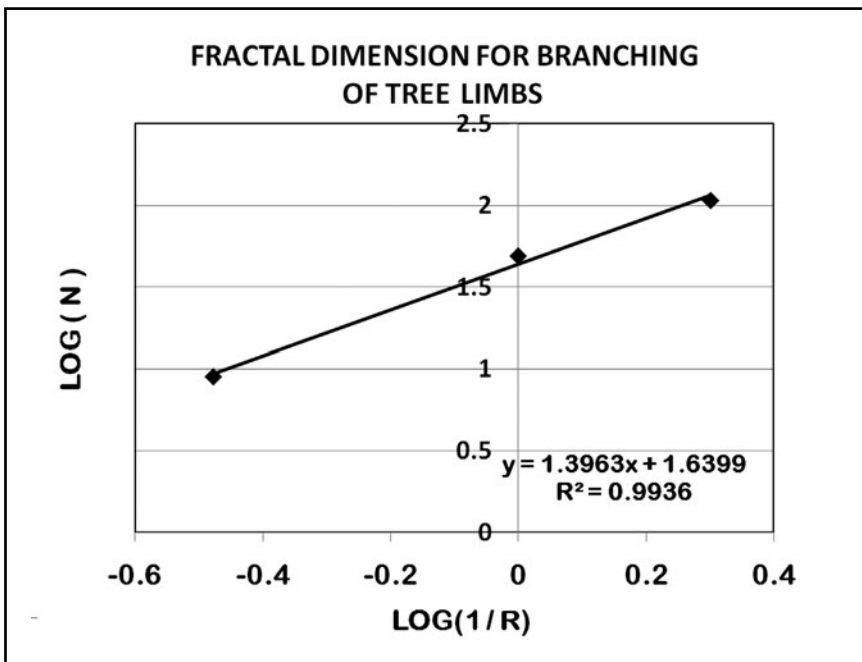


Illustration 8.9

As the slope on the graph in illustration 8.9 demonstrates, the fractal dimension for this particular example is about 1.40.

Branching of tree limbs has similar analogies in anatomy. The branching of the airways in the lungs, the branching of veins and the arterial systems in the human body, and nerves in the nervous system could be analyzed by using fractal dimensions. One motivation for examining human anatomy by using fractals is that abnormalities in between segments of organs and between individuals might be uncovered with better speed, accuracy, and consistency than by using conventional methods.

8.3 APPLICATIONS OF FRACTALS TO HUMAN ANATOMY

The branching of airways in the lungs is a self-replicating process, which is similar to the branching of trees. See illustration 8.10 for an example of this process.

The best clinical image of the lungs is provided by a CT scanner in which a lung display window and level is used. This is shown in illustration 8.11.

There are two different methods to determine the fractal dimensions from the data in the lung CT scan. The first method is to use the box counting approach that was used in the example with tree branches. In this case, some criteria must be utilized to determine whether or not a box gets counted. The

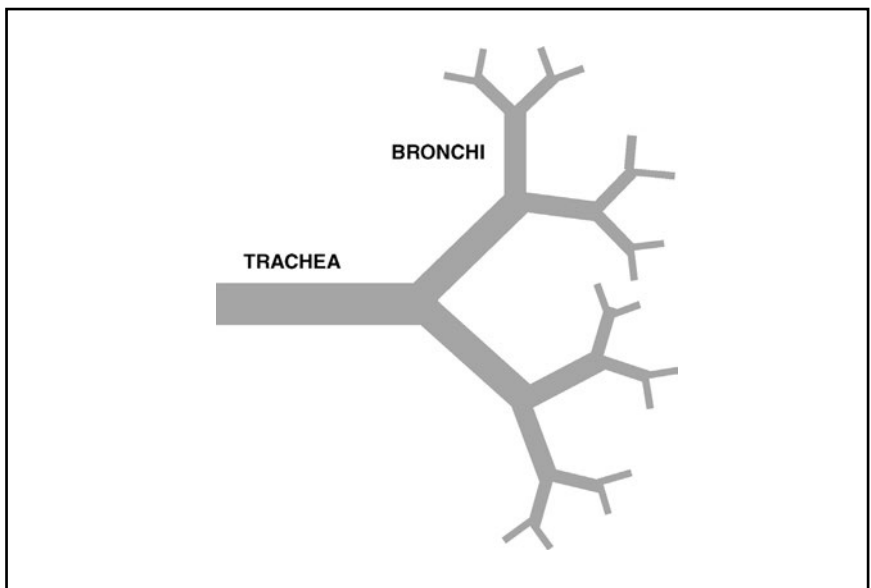


Illustration 8.10. Branching in bronchi of lungs, which looks like fractals.

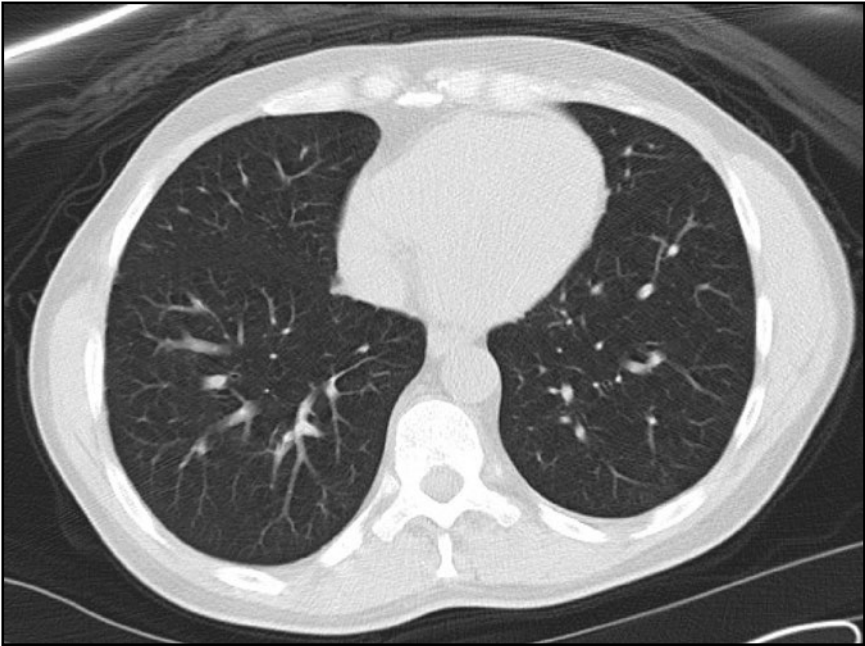


Illustration 8.11

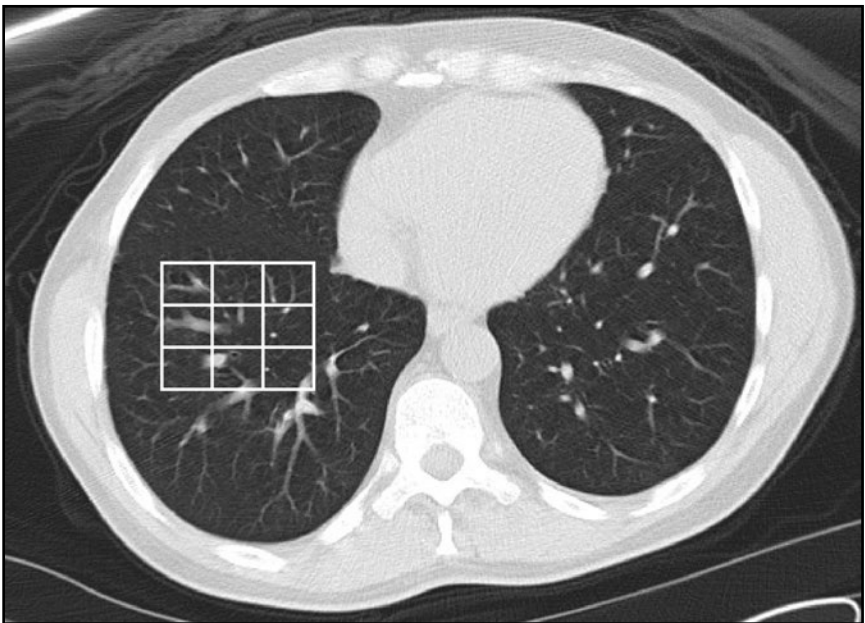


Illustration 8.12

observer needs to select a CT number threshold for the counting criteria. For this example, any box which had an average CT number in the region of interest greater than -800 Hounsfield Units (H.U.) was counted. Boxes with the average CT number inside the box of less than -800 H.U. were not counted. This process is shown in illustration 8.12.

The problem with this approach is that the lung values vary with location within the lung and from one CT slice to the other. A detailed analysis would evaluate each section of the lung and each CT slice. For the purposes of this example, the data from the regions shown were measured and plotted as a graph of $\text{Log} (N)$ versus $\text{Log} (1/R)$ in illustration 8.13.

From the box counting approach, the fractal dimension of the lung region in the given CT slice is the slope of the graph (trend line), or 1.953.

Another approach would be to measure the mass in a series of concentric circles in the same location. Circular regions of interest can be easily determined from the CT scanner data. The area of the circular regions of interest can be used to find the radii of the concentric circles:

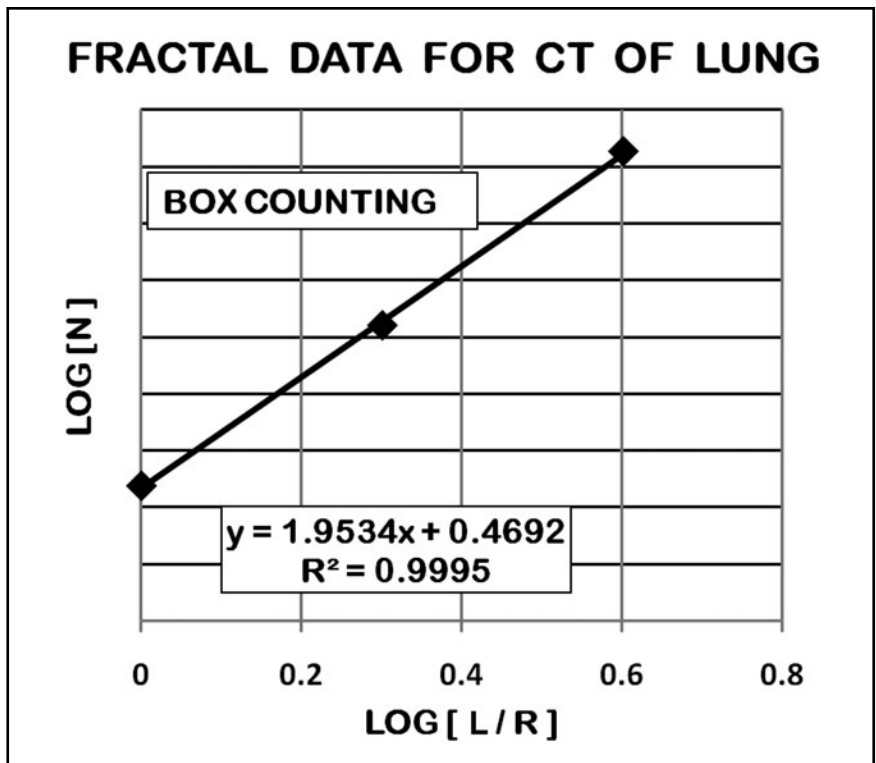


Illustration 8.13

$$\text{Radius} = \left[\text{Area} / \pi \right]^{0.5}. \quad (8.10)$$

The density of tissue in the regions of interest (ROIs) can be approximated by the following equation:

$$\text{Density} = (0.001 * \text{mean CT\#}) + 1.0 \text{ g/cc} \quad (8.11)$$

The mass of the tissue could then be calculated by the expression given below:

$$\text{Mass} = (\text{slice thickness}) * (\text{density}) * (\# \text{ pixels in the ROI}). \quad (8.12)$$

Using this procedure, concentric circular ROIs were placed on the same section of the lung CT slice. The data were obtained, and the radius and mass for each concentric circle were determined. It is assumed that the relationship between (Mass) and (Radius) of each concentric circle is a power function.

$$\text{Mass} = \text{constant} * (\text{Radius})^D \quad (8.13)$$

Therefore, by taking logarithms of both sides of the equation and rearranging terms:

$$D = \frac{\text{Log}(\text{Mass})}{\text{Log}(\text{Radius})} + \text{constant}. \quad (8.14)$$

D is the fractal dimension for this mass method of analysis. In the graph shown in illustration 8.14, the slope of the graph of Log (Mass) versus Log (Radius) is the fractal dimension.

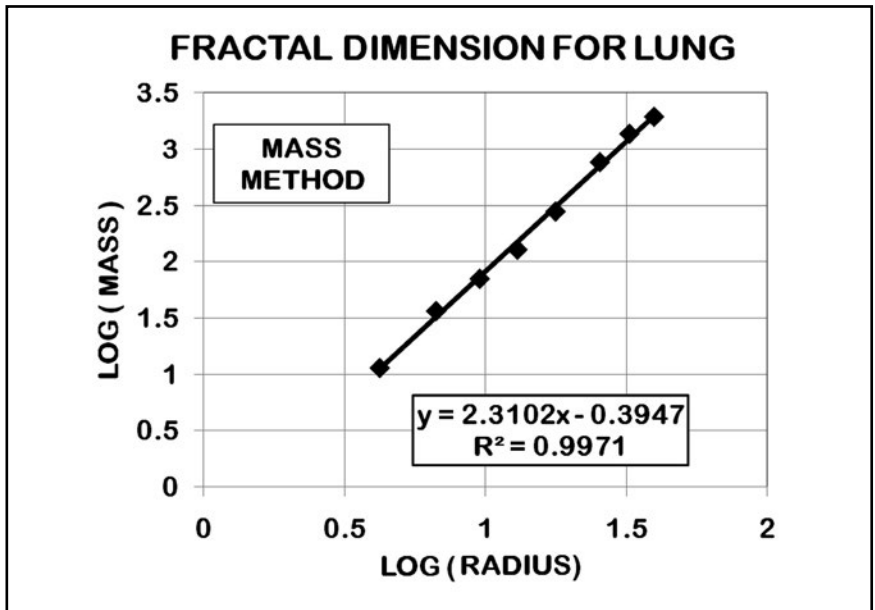


Illustration 8.14

Slightly different fractal dimensions are obtained by the two methods. Regardless, a value of about 2.0 for the fractal dimension indicates the branching structure of the vessels occupies much of the space for the tissue in the lungs. This type of analysis can be used for other anatomical structures in the body.

8.4 MANDELBROT SETS

To continue with the topic of self-replicating figures, mathematical processes can produce graphs with patterns. Standard polynomials only generate graphs of various continuous curves. However, by using complex numbers, more interesting figures can be generated. A complex number has a real number, which is plotted along the abscissa (x -axis), and an imaginary number, which is plotted along the ordinate (y -axis). The square root of -1.0 is an imaginary number that is given the symbol i . Hence, a complex number can be written in the following form:

$$Z = (a) + i(b) \quad \text{where } a \text{ and } b \text{ are real numbers.} \quad (8.15)$$

A sequence of complex numbers is generated from a starting complex polynomial. The number that is computed is then substituted into the original complex polynomial, and the process is continued many times. Mathematically, the process can be written as the following expression:

$$Z_{n+1} = (Z_n)^2 + C. \quad (8.16)$$

Each Z and each C is a complex number. This method is used to generate each subsequent number starting from an initial “seed” number, usually designated C . The selection of the appropriate C starting term is important. For many C values, the self-replication sequence either becomes infinitely large or very small, approaching zero. Varying the value of C produces a vast variety of different graphs. Values of C that produce figures with finite boundaries are called *Mandelbrot sets*. If the graphs of the complex numbers produced by this process are connected with a line, interesting figures can be

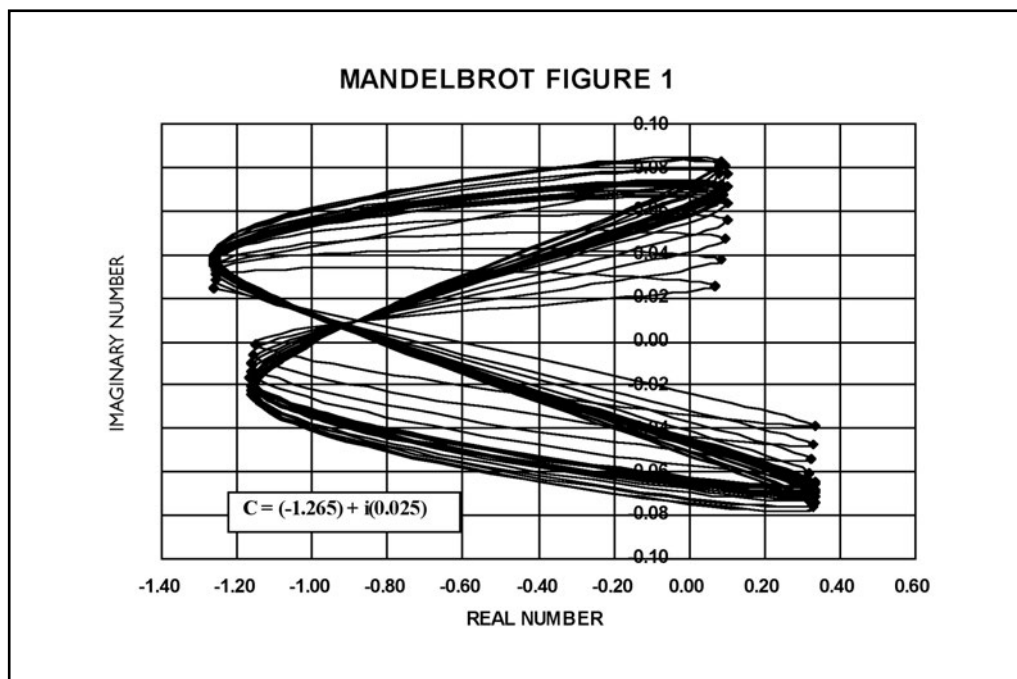


Illustration 8.15

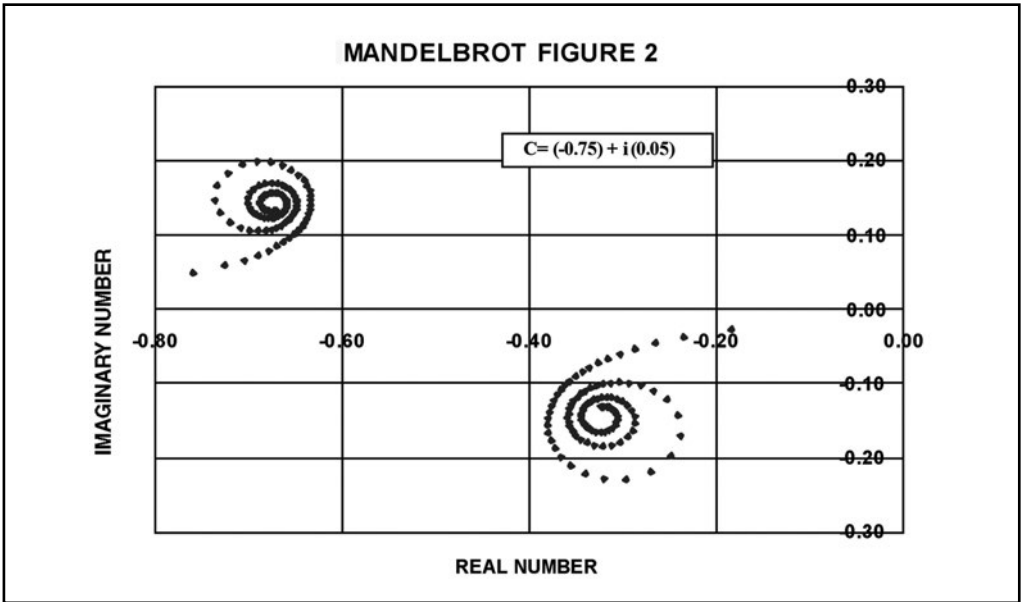


Illustration 8.16

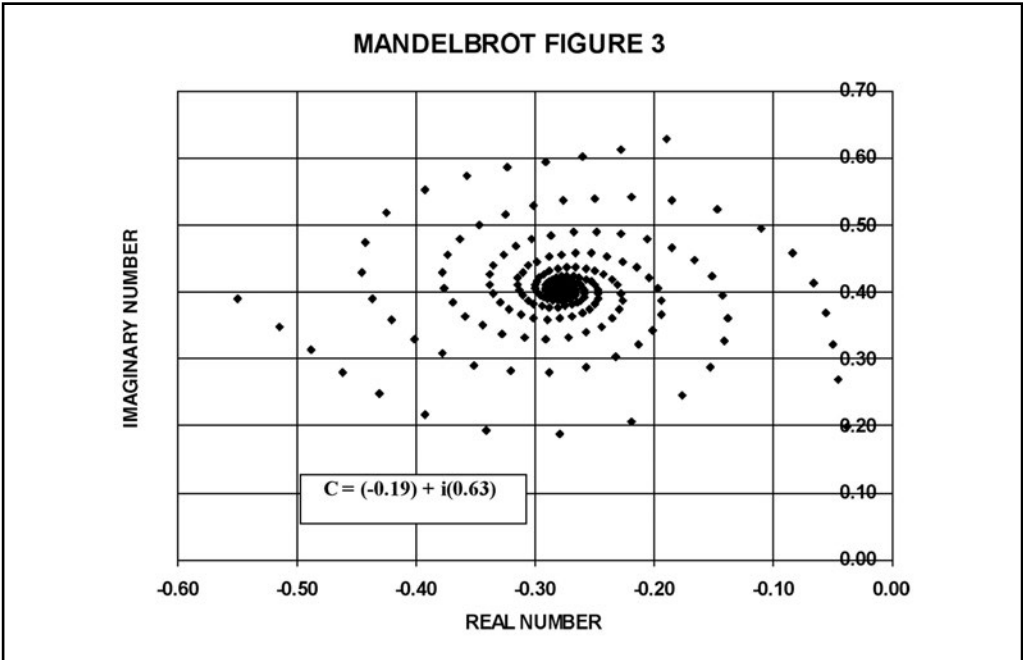


Illustration 8.17

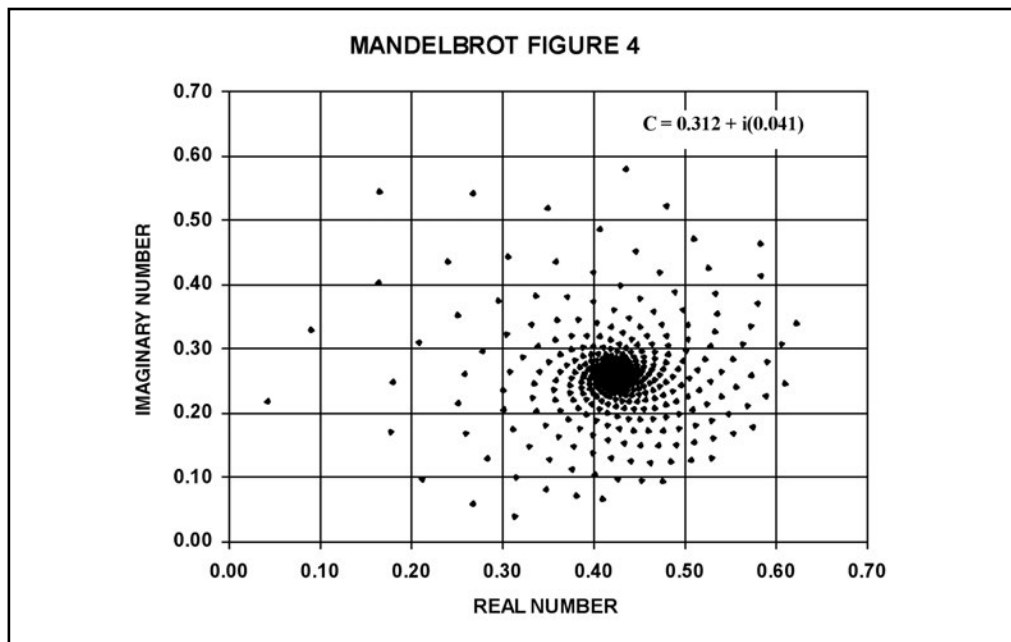


Illustration 8.18

produced. Selection of C equal to $(-1.265) + i(0.025)$ produces a figure that looks like a series of concentric butterflies, as shown in illustration 8.15.

Interesting graphs are also produced by just plotting the points generated by the selection of various seed values for C . Three different Mandelbrot figures are shown in illustrations 8.16 through 8.18; each was generated by a different value for C .

Mandelbrot figure 2 has the appearance of snail shells. Mandelbrot figures 3 and 4 look like the spiral shape of stars in a galaxy. In any event, these complex polynomials can be used to generate self-replicating series of values that have very interesting appearances. Small changes in the values of the numbers in C have a dramatic change in the appearance of the figures.

Mandelbrot had an interesting way to present the various values of C that give figures with bounded values. Mandelbrot plotted the values of C that gave a bounded series on a complex graph. These values of C produced a very interesting figure. These sets of values of C that give bounded self-replicating series are called *Mandelbrot sets*. Other higher-order polynomials

can also be used to generate interesting figures and their seed values of C can also be plotted as a graph.

USEFUL REFERENCES

Barnsley, M. F. *Fractals Everywhere*, 2nd edition. San Diego, CA: Academic Press, 2000.

Briggs, J. *Fractals: The Pattern of Chaos: Discovering a New Aesthetic of Art, Science and Nature*. New York: Simon & Schuster, 1992.

Falconer, K. J. *Techniques in Fractal Geometry*. West Sussex, England: John Wiley & Sons Ltd., 1997.

Falconer, K. J. *Fractal Geometry: Mathematical Foundations and Applications*. West Sussex, England: John Wiley & Sons Ltd., 2003.

Gleick, J. *Chaos: Making a New Science*, 2nd edition. New York: Penguin Books, 2008.

Leibovitch, L. S. *Fractals and Chaos: Simplified for Life Sciences*. New York: Oxford University Press, Inc., 1988.

Mandelbrot, B. B. *The Fractal Geometry of Nature*. New York: W. H. Freeman, 1983.

Mandelbrot, B. B. *Fractals and Chaos: The Mandelbrot Set and Beyond*. New York: Springer-Verlag New York Inc., 2004.

Peterson, I. *The Mathematical Tourist: New and Updated Snapshots of Modern Mathematics*. New York: Barnes & Noble Books, 2001.

Schroeder, M. *Fractals, Chaos, Power Laws: Minutes from an Infinite Paradise*. Mineola, NY: Dover Publications, 2009.

PRACTICE EXERCISES

1. On a square, divide each side into three parts. On each center segment, add another square that has sides that are one-third the length of the original square. Repeat this process two more times. What is the area encompassed by the new figure? How many line segments are on the circumference of the new figure? How does the length of circumfer-

ence of the new figure compare with the original figure? What is its fractal dimension?

2. Obtain a picture of a tree that has lost its leaves. Use the box counting method to determine its fractal dimension. What is this value of the fractal dimension? Is this a value that you would expect?
3. Obtain a picture of the coastline of Ireland. Use the box counting method to determine its fractal dimension. Try to find an article that computes Ireland's fractal dimension. How well do the calculations compare with the published value? If the coastline is more complex, does the fractal dimension increase or decrease? Why is this important?
4. Obtain a picture of the venous blood vessels in the leg. Use the box counting approach to determine the fractal dimensions. What is the mathematical description of the repetition pattern of the branching? Why is this important? If the value of the fractal dimension decreases, what does it mean from a physiological viewpoint?
5. Obtain a CT scan image with a slice through the kidneys that can be analyzed for its CT numbers. Use the density approach described in this book to determine its fractal dimensions. What is this fractal dimension? If the value is found to be greater in other patients, what does this indicate clinically?
6. Create a graph of a Mandelbrot set using the starting value of $C = (-0.25) + (0.96) i$. Continue the process through at least 100 terms. Plot the points and connect the points with lines. Change the values for C slightly to obtain another figure.
7. Create a picture of a tree by using a repeating branching process where the branches are one-half the length of the original tree trunk. What is the mathematical description of the branching process that was used? How might the tree be made more realistic?
8. Create a sequence of numbers using a polynomial feedback loop of $X_{n+1} = K * X_n * (1 - X_n)$ where K is a constant. Let $K = 1.15$ and let the starting value of $X_0 = 0.11$. Plot X_{n+1} on the ordinate axis versus X_n on the abscissa axis. Describe the appearance of the graph. Does the graph have a maximum? Is there anything in the medical or medical physics worlds that could be described with a feedback loop?

9. Create an interesting image starting with a rectangle and using a rule in which smaller rectangles are subtracted from the original rectangle. Describe the rule in detail. Provide the image of the resultant figure after five iterations. If the process were to continue infinitely, what would be the area remaining from the original figure? What would be the number of line segments used to form the figure? What would be the fractal dimension?

10. Explain how fractals might be useful in other sciences like astronomy, zoology, and chemistry. Give a detailed example. What is the overall benefit of fractals? How does the universe look from a small-scale prospective?

Index

Note: Page numbers followed by f refer to figures; page numbers followed by t refer to tables.

- accuracy of a test, 80
- activity of a radioisotope, 21, 128–131, 129f, 129t, 130f, 131f
- ambiguous survey data, 245
- appointment schedules, 198–202, 199f, 200f, 201f, 202f
- attenuation coefficient, linear, 205–206, 205f, 206t
- Automatic Exposure Control (AEC), 125
- average. *See* central tendency; mean
- Bayes' Theorem, 97–108
 - applications of, 103–108
 - to cancer risk from CT, 106–108
 - to drug testing, 103–104, 244
 - to mammography screening, 104–105
 - basic concepts of, 97–99
 - population characteristics and, 99–102, 100f, 102f, 244
- bell curve. *See* Normal (Gaussian) probability distribution
- biased sampling, 240–241, 243
- bi-modal frequency distribution, 7
- binomial probability distribution, 18–25
 - applications of
 - to CT scanner downtime, 22–23, 23f
 - to isotopic decay, 22, 24–25, 25f
 - to mammography screening, 23–24
 - fundamentals of, 18–22, 20f, 20t, 21f
 - mean of, 26
 - Poisson distribution and, 25–26
- blood pressure measurements
 - Chi-Square Test with, 88
 - dividing into two groups, 76–78, 77f, 79f, 80
 - ROC graph for, 82, 83f, 83t, 84
 - in flawed experiments, 240–241, 245–246
- blur, 222, 223f, 224–225, 226, 227
- box counting method of fractal analysis, 172, 173f, 174f
- for lung CT, 175, 176f, 177, 177f
- branching structures, fractal analysis of, 171–172, 173f, 174f, 175
- calibration
 - errors in, 245–246
 - of ionization chambers, 90–92, 91t
- cataracts, radiation-induced, 43–44
- causation, fallacious inference of, 155–156, 156f, 240, 241f, 244
- central tendency, 6–7, 17. *See also* mean; median; mode
 - inappropriate use of, 238–239, 238f, 239f
- central two-tailed cumulative probability, 60, 61f. *See also* two-tailed cumulative probability distribution
- characteristic curve, for film-screen systems, 43, 66, 67–68, 69f, 70
- Chauvenet's criterion, 87–88, 88t

- chest imaging
 fractal analysis of, 175–178, 175f, 176f, 177f, 179f
 noise in, 216f
- Chi-Square Test, 88–90, 89f, 90t
- cluster sampling, 51
- CNR. *See* contrast-to-noise ratio (CNR)
- coastlines, fractal, 169, 170f, 171, 172f
- Coefficient of Alienation, 155
- Coefficient of Determination, 155
- Coefficient of Non-Determination, 155
- coherent scatter, 204f, 205–207, 206t, 207f
- coin toss, 18–21, 20f, 20t, 21f
- collisions, molecular, 190, 191–192
- combinations, 2–4, 3f, 4t
- complementary error function (ERFC), 41
- complex numbers
 defined, 179
 iterated sequences of, 179–182, 180f, 181f, 182f
- Compton scatter, 204f, 205–210, 206t, 207f
 angular dependence, 207–209, 208f, 209f
 photon energy, 208–209
- computed radiography (CR), noise in, 216f
- computed tomography. *See* CT (computed tomography)
- conditional probability, 97–99. *See also* Bayes' Theorem
- confidence intervals, 60, 64–66, 65f, 65t
 applications of
 to CT radiation dose, 92–93
 to mammography radiation dose, 70–71
 for linear regression, 137–138, 140, 141f
 for mean value, 66, 70, 76
 with one-tailed distribution, 66, 71
 in quality control, 246
- confounding factors, 241, 244
- continuous frequency distribution, 5
- contrast agent, in digital subtraction angiography, 227–232, 229f, 230f
- contrast agent toxicity
 Chi-Square Test for age hypothesis, 89–90, 90t
 Log Normal distribution of, 37–38, 37t, 38f, 66
- contrast-detail diagrams, 220–225, 222f
- contrast-to-noise ratio (CNR), 217–220, 218f, 219f
 blur and, 222, 224–225
 in digital subtraction angiography, 228–232
 size of low-contrast object and, 221, 225
- control group, 240–241
- correlation
 for linear functions. *See* correlation coefficient
 for nonlinear functions, 157
 spurious, 155–156, 156f, 240, 241f, 244
- correlation coefficient, 149–151
 alternative form for, 151–153
 application of, 153, 154–155
 causal relationship and, 155–156, 156f, 240, 241f
 significance of, 153–155
 table for, 269–273
 terminology for, 155
 T_C test for, 153–154, 155, 270
- CR (computed radiography), noise in, 216f
- CT (computed tomography)
 blur in, 222
 lung, fractal analysis of, 175–178, 175f, 176f, 177f, 179f
 radiation dose from
 cancer caused by, 106–108, 243
 confidence limits for, 92–93
 to head, 32–34, 33f, 33t, 34f, 106–107
 number of measurements, 86–87
 scanner downtime, 22–23, 23f
 signal-to-noise ratio in, 216–217
- CTDI (computed tomography dose index), 32–34, 33f, 33t, 34f
 cancer risk and, 106
 confidence limits for, 92–93
 number of measurements, 86–87
- cumulative frequency distribution, 7–8, 8f
- cumulative probability distributions. *See* Log Normal probability distribution, cumulative; Normal (Gaussian) probability distribution, cumulative; one-tailed cumulative probability

- distribution; two-tailed cumulative probability distribution
- curve fitting. *See* least squares method
- decay constant, 21, 24
- decay rate, 21–22, 24–25, 25f
- decision matrix, 77–81, 78t, 79t, 80t
 - in Bayesian analysis, 99, 103, 107
- degrees of freedom (df)
 - Chi-Square Test and, 89, 89f, 90
 - T*-test and, 85, 265–267
- Detective Quantum Efficiency (DQE), 225–227
- digital imaging systems. *See also* image quality
 - signal-to-noise ratio of, 216f, 217
- digital subtraction angiography (DSA), 227–232, 229f, 230f, 232f, 233f
- discarding data, 87–88, 88t, 241, 244–245
- discrete frequency distribution, 4t, 5, 5f
- dispersion of probability distribution, 17, 17f. *See also* standard deviation (SD or σ)
- distributions. *See* frequency distributions; probability distributions
- dose. *See* contrast agent toxicity; radiation dose
- downtime, CT scanner, 22–23, 23f
- DQE. *See* Detective Quantum Efficiency (DQE)
- drug screening, 103–104, 244
- DSA. *See* digital subtraction angiography (DSA)
- edge enhancement algorithms, 215
- efficiency of image receptor, 225–226
- electronic components
 - cluster sampling of, 51
 - cumulative failure of, 43
 - time to failure of, 35, 36f
- electronic noise, 190–191, 191f, 215, 226
- equally likely outcomes, 13, 14f
- ERFC (complementary error function), 41
- Error Function (ERF), 38–43, 41f, 43f, 60. *See also* Normal (Gaussian)
 - probability distribution, cumulative applied to cataract risk, 43–44
 - table of, 255–257
- Excel spreadsheet
 - Chi-Square Test with, 89
 - of head CT radiation doses, 33–34, 34f
 - random number generator of, 188, 189f, 190, 194
 - T*-test with, 85
- experiments, poorly designed, 240–242, 244–245
- exponential functions, 127–131
 - correlation for, 157
 - least squares fitting with, 130, 132
 - logarithmic functions and, 132
 - processes represented by, 127
- exposure from x-ray tube, 57–59, 58t, 59t, 70
- factorials
 - gamma function and, 265
 - Stirling approximation to, 27
- False Negatives (FN), 78–81, 79f, 79t, 80t
 - conditional probability and, 97, 99
- False Positives (FP), 78–81, 79f, 79t, 80t
 - conditional probability and, 97, 99
 - ROC graphs and, 82–84, 83f, 83t
- fences, 64–66, 65f. *See also* confidence intervals
- film-screen systems
 - characteristic curve for, 43, 66, 67–68, 69f, 70
 - signal-to-noise ratio of, 216–217
- flood-field image, 220
- fourth moment of probability distribution, 16
- fractal dimension, 164–166, 169
 - by box counting method, 172, 173f, 174f
- fractals
 - applications of
 - to branching structures, 171–172, 173f, 174f, 175
 - to coastlines, 169, 170f, 171, 172f
 - to lung CT, 175–178, 175f, 176f, 177f, 179f
 - basic concepts of, 163–169, 163f, 165f
- frequency distributions, 4–6, 4t, 5f, 6f
 - bi-modal, 7
 - cumulative, 7–8, 8f
 - measures of central tendency for, 6–7
- full width at half maximum (FWHM), 30

- gamma function, 265
- Gaussian distribution. *See* Normal (Gaussian) probability distribution
- Geiger-Mueller detector, 27–29, 28f, 29f, 29t
- Golden Ratio, 117–119, 117t, 118f
- goodness of fit, Chi-Square Test for, 88–90, 89f, 90t
- grades of students, distribution of, 31–32, 32t
- graphical fits to data. *See* least squares method
- half-life, of radioisotope, 21, 24
- height vs. age of boys
correlation coefficient for, 153, 154–155
linear regression of, 138–140, 138t, 139t, 141f
- histogram, 4, 5f
- hypothesis testing, with Chi-Square Test, 88–90, 89f, 90t
- identity matrix, 121
- image processing, 215
- image quality
blur, 217, 222, 223f, 224–225, 226, 227
contrast-to-noise ratio, 217–220, 218f, 219f, 221, 222, 224–225
in digital angiography, 228–232
Detective Quantum Efficiency (DQE), 225–227
Noise Equivalent Quanta (NEQ), 226, 227
radiation dose and, 216–217, 227
signal-to-noise ratio, 215–217, 216f, 225–227
in digital angiography, 228–229, 231–232
size of low-contrast objects and, 220–222, 222f, 225
sources of noise, 215, 226–227
- Index of Correlation, 157
- intensifying screens. *See* film-screen systems
- inverse matrix
calculation of, 121–122
in linear regression, 119–123
in second-degree curve fitting, 125–126
- ionization chambers, calibration of, 90–92, 91t
- Koch snowflake, 166, 168f, 169
- Kurtosis, 16–17
- least squares method. *See also* linear regression
for linear fit, 112–119
with exponential data, 130, 132
with logarithmic data, 132
with power function, 135
using inverse matrix, 119–123
for polynomial fit, 123–126, 125t, 127f
- leptokurtic distribution, 17
- linear attenuation coefficient, 205–206, 205f, 206f
- linear correlation coefficient. *See* correlation coefficient
- linear regression. *See also* correlation coefficient; least squares method; standard error of the estimate (SE)
basic concepts of, 111–119
confidence intervals for, 137–138, 140, 141f
example of Golden Ratio, 117–119, 117t, 118f
for exponential data, 128, 130–131, 130f, 131f, 132
inverse matrix approach to, 119–123
for logarithmic data, 131–132
- line spread function (LSF), 224
- logarithmic functions, 131–132
correlation for, 157
- Logit Transform, 66–70, 69f
- log-log graph, 132–133
application of, 133–135, 133t, 134f
- Log Normal probability distribution
applied to toxicities, 37–38, 37t, 38f, 66, 67, 68f
cumulative, 66, 67, 68f
fundamentals of, 34–36, 36f
- lower one-tailed cumulative probability distribution, 42–43, 42f, 43f, 60, 61f
applied to cataract risk, 44
sigmoid curves and, 43, 43f, 66

- table of values, 259–263
- LSF (line spread function), 224
- lung CT, fractal analysis of, 175–178, 175f, 176f, 177f, 179f
- mammography
 - average glandular dose, 70–71, 92, 124–126, 125t, 127f
 - screening with, 23–24, 79, 104–105
- Mandelbrot sets, 179–182, 180f, 181f, 182f
- mask, angiographic, 228, 230, 230f, 231, 232, 233f
- mass attenuation coefficients, 204f, 205–206, 206t
- matrix multiplication, 119–120
- mean, 6–7. *See also* standard error of the mean (SE)
 - of binomial distribution, 26
 - inappropriate use of, 238, 239, 239f
 - of Normal distribution, 29–30, 49–50, 53t
 - of Poisson distribution, 26–27, 53–54
 - of population, 30, 51, 52
 - of sample, 30, 51–52
 - sample size and, 52, 86–87, 92, 196–198, 197f, 197t
 - variation of, 75–76
 - of skewed probability distribution, 14, 15, 16
 - weighted, 50
- median, 6, 7, 8
 - inappropriate use of, 238–239, 238f
 - of Normal distribution, 49
 - of skewed probability distribution, 14, 15, 16
- mesokurtic distribution, 17
- mining data, 245
- misuse of statistics, 237–246
 - categories of, 242–246
 - introduction to, 237–242, 242f
- mode, 6, 7
 - dispersion and, 17
 - of Normal distribution, 49
 - of skewed probability distribution, 14, 15, 16
- modulation transfer function (MTF), 224–225, 226, 227
- molecular collisions, 190, 191–192
- Monte Carlo methods
 - applications of
 - mean value variation, 196–198, 197f, 197t
 - scheduling appointments, 198–202, 199f, 200f, 201f, 202f
 - x-ray photon interactions, 203–210
 - basic process in, 192, 194–196, 195f
 - random numbers for, 187–190, 189f
 - trials (histories) in, 196
- Negative Predictive Value (NPV), 81
- noise. *See* contrast-to-noise ratio (CNR); electronic noise; image quality; quantum mottle; signal-to-noise ratio (SNR)
- Noise Equivalent Quanta (NEQ), 226, 227
- Normal (Gaussian) probability distribution
 - Chauvenet's criterion and, 88
 - cumulative, 38–43, 40f, 41f, 42f, 43f
 - approximation to, 62–63, 63t, 64f
 - confidence intervals and, 60, 64–66, 65f, 65t, 71, 76
 - four types of, 60, 61f, 62f
 - in Monte Carlo method, 194–196, 195f, 200
 - table of values, 255–257
 - Z value and, 84–85, 85t
- fundamentals of, 29–31, 31f
- image contrast and, 219, 219f
- mean of, 29–30, 49–50, 53t
- questionable applications of
 - to head CT radiation dose, 32–34, 33f, 33t, 34f
 - to student grades, 31–32, 32t
- separation of two populations, 76–77, 77f
 - Z parameter and, 84–85, 85t, 91
- skewed example compared to, 32–34, 33f, 34f
- standard deviation of, 29, 30–31, 31f, 50–51, 52, 53t
 - confidence intervals and, 64–66, 65f, 65t
 - cumulative probability and, 62–63, 63t, 64f

- Normal (Gaussian) probability distribution
(continued)
 table of values, 249–254
T distribution compared to, 85, 266, 269
 variance of, 50–51, 53t
- nuclear medicine. *See also* radioactive decay
 contrast-to-noise ratio in, 220
 quantum mottle in, 216
 signal-to-noise ratio in, 71
- one-tailed cumulative probability
 distribution, 41–43, 42f, 43f, 60, 61f, 62f
 applied to cataract risk, 44
 confidence level for, 66, 71
 in random number generation, 195
 sigmoid curves and, 43, 43f, 66, 195
 table of values, 259–263
T-test and, 86, 267
Z value and, 84
- optical transfer function (OTF), 224
- peakedness of probability distributions, 16–17
- permutations, 1–2, 2f, 3, 3f, 4t
- photoelectric effect, 204f, 205–207, 206t, 207f
- pixel shifting, 228
- platykurtic distribution, 17
- Poisson probability distribution, 25–29
 Chauvenet's criterion and, 87
 fundamentals of, 25–27
 Geiger-Mueller detector and, 27–29, 28f, 29f, 29t
 mean of, 26–27, 53–54
 standard deviation of, 52–54
- polynomial fit to data, 123–126
 Index of Correlation for, 157
- population. *See also* separation of two populations
 mean of, 30, 51, 52
 standard deviation of, 30, 51, 52
- Positive Predictive Value (PPV), 81
- power functions, 132–133
 application of, 133–135, 133t, 134f
 correlation for, 157
- probability distributions, 13–17. *See also*
 binomial probability distribution;
 cumulative probability distributions;
 Log Normal probability distribution;
 Normal (Gaussian) probability
 distribution; Poisson probability
 distribution; skewed probability
 distributions; *T* distribution
- product moment coefficient, 150
- quality control, confidence intervals in, 246
- quality of image. *See* image quality
- quantum mottle, 215, 216, 226
 in digital subtraction angiography, 228, 229f, 230
- quartile deviation (QD), 16
- quartiles, 7, 8
- questionnaires, poorly designed, 246
- radiation detector, Geiger-Mueller, 27–29, 28f, 29f, 29t
- radiation dose
 ambiguous survey of, 245
 from CT scans
 cancer caused by, 106–108, 243
 confidence limits for, 92–93
 to head, 32–34, 33f, 33t, 34f, 106–107
 number of measurements of, 86–87
 cumulative probability of bioeffect, 42
 image quality and, 216–217, 227
 to laboratory workers' thyroids, 56, 86
 to lens of eye, 43–44
 in mammography, 70–71, 92, 124–126, 125t, 127f
 Monte Carlo calculations of, 203, 210
 whole-body, 66
- radiation exposure from x-ray tube, 57–59, 58t, 59t, 70
- radioactive decay, 21–22, 24–25, 25f
 graphical fit to data, 127–131, 129f, 129t, 130f, 131f
 scintillation counter and, 54–55, 54t
- RAND(), 188, 189f, 190, 194
- random numbers, 187–190, 189f
- random sampling, 51

- random walk, 190–192, 191f, 193f, 194f
- Receiver Operating Characteristic (ROC) graphs, 82–84, 83f
- relative frequency distribution, 5–6, 6f
- cumulative, 7–8, 8f
 - measures of central tendency, 6–7
 - weighted mean, 50
- relative standard deviation (RSD), 54–55, 54t
- sample
- discarding data from, 87–88, 88t, 241
 - representative of population, 75–76
- sample mean, 30, 51–52. *See also* standard error of the mean (SE)
- sample size and, 52, 86–87, 196–198, 197f, 197t
 - variation of, 75–76
- sampling, 51–52
- sampling error, 240–241, 243
- scattered radiation
- coherent, 204f, 205–207, 206t, 207f
 - Compton scatter, 204f, 205–210, 206t, 207f
 - angular dependence, 207–209, 208f, 209f
 - photon energy, 208–209
- scheduling appointments, 198–202, 199f, 200f, 201f, 202f
- scintillation camera, flood-field image with, 220
- scintillation counter, standard deviation for, 54–55, 54t
- SD. *See* standard deviation (SD or σ)
- SE. *See* standard error of the estimate (SE); standard error of the mean (SE)
- semilogarithmic graph, 128, 130–131, 130f, 131f, 132
- sensitivity of a test, 80, 99–100, 101, 102, 244
- separation of two populations, 76–77, 77f
- applications of, 90–93, 91t
 - decision matrix and, 77–81, 78t, 79t, 80t
 - ROC graphs and, 82–84, 83f
 - T*-test for, 84–86
 - application of, 90–92, 91t
 - table of values, 265–267
- Z* parameter and, 84–85, 85t
- Sierpinski triangle, 166, 167f
- sigmoid curves, 43, 43f, 66
- Logit Transform and, 66–70, 68f, 69f
 - in random number generation, 195
- signal-to-noise ratio (SNR), 71–72, 215–217, 216f
- Detective Quantum Efficiency and, 225–227
 - in digital subtraction angiography, 228–229, 231–232
- skewed probability distributions, 14, 14f, 15–16, 15f
- inappropriate analysis of, 238–239, 238f
- Log Normal. *See* Log Normal probability distribution vs. Normal distribution, 32–34, 33f, 34f
- skewness, 16, 34f
- smoothing algorithms, 215
- snowflake, 166, 168f, 169
- spatial frequency of image, 224–225, 227
- specificity of a test, 81, 99, 101, 102, 244
- standard deviation (SD or σ), 17
- for added or subtracted data, 55–56, 55f
 - inappropriate use of, 238
 - for multiplied or divided data, 56–58, 58t, 59t
 - of Normal distribution, 29, 30–31, 31f, 50–51, 52, 53t
 - confidence intervals and, 64–66, 65f, 65t
 - cumulative probability and, 62–63, 63t, 64f
 - of Poisson distribution, 52–54
 - relative, 54–55, 54t
 - of sample vs. population, 30, 51, 52
 - skewness in terms of, 16
- standard error of the estimate (SE), 135–138
- application of, 138–140, 138t, 139t, 141f
 - correlation coefficient in terms of, 152
- standard error of the mean (SE), 59, 75–76
- confidence levels for, 66, 70
 - with Monte Carlo method, 196–198, 197f

- standard error of the mean (SE), 59, 75–76
(*continued*)
Student's *T*-test and, 84–86
Z values and, 84–85, 86
- standard error of *Y*, for nonlinear fit to
data, 157
- statistics
beneficial uses of, 246
misuse of, 237–246
- Stirling approximation, 27
- stratified sampling, 51
- Student's *T*-test. *See T*-test
- surveys, poorly designed, 245, 246
- symmetrical probability distribution, 15,
15f, 16
- systematic measurement errors, 241,
245–246
- systematic sampling, 52
- T* distribution, 265–266
- tolerances, 60. *See also* confidence
intervals
- toxicities, Log Normal distribution of,
37–38, 37t, 38f, 66, 67, 68f
- True Negatives (TN), 78–81, 79f, 79t, 80t
conditional probability and, 97
- True Positives (TP), 78–81, 79f, 79t, 80t
conditional probability and, 97
ROC graphs and, 82–84, 83f, 83t
- T*-test, 84–86
for ionization chamber calibration,
90–92, 91t
table of values, 265–267
- T_c test for correlation coefficient,
153–154, 155, 270
- two-tailed cumulative probability
distribution, 20–21, 21f, 60, 61f
confidence intervals for, 64–66, 65f, 65t
Error Function as, 39–41, 41f
Poisson, 29, 29f, 29t
in random number generation, 194–196,
195f
- table of values, Normal, 255–257
T-test and, 85, 266
Z value and, 84
- unsharpness. *See* blur
- upper one-tailed cumulative probability
distribution, 60, 62f
confidence level for, 66, 71
- variance (σ^2)
of Normal distribution, 50–51, 53t
of Poisson distribution, 53
- waiting times, 198–202, 199f, 200f, 201f,
202f
- weighted mean, 50
- weighting factor, 50
- well scintillation counter, standard
deviation for, 54–55, 54t
- white noise, 216
- Wiener Noise, 227
- x-ray film-screen systems. *See also* image
quality
characteristic curve for, 43, 66, 67–68,
69f, 70
signal-to-noise ratio of, 216–217
- x-ray imaging
contrast-to-noise ratio in, 220
signal-to-noise ratio in, 216–217, 216f
- x-ray photon interactions, 203–210
- x-ray tube
energy spectrum of, 203, 204f
exposure from, 57–59, 58t, 59t, 70
focal spot blur with, 222
output vs. kVp, 133–135, 133t, 134f
reproducibility assessment of, 52, 53t,
70
- Z parameter, 84–85, 85t, 86–87
correlation coefficient and, 153–154

About the Author

Dr. Edward L. Nickoloff completed his B.S. degree in Physics from Lebanon Valley College in Annville, Pennsylvania, and his M.S. degree in Nuclear Physics from the University of New Hampshire in Durham, New Hampshire. After his M.S. degree, Dr. Nickoloff worked in the electronic industry for 6 years. Then, due to the death of his mother Pearl from cancer, he wanted to work and do research in the medical field. To pursue this goal, he returned to graduate school; he received his D.S. degree with Distinction in Medical Physics from Johns Hopkins University, Baltimore, Maryland. Even prior to graduation, Dr. Nickoloff was hired by the Department of Radiology at the Johns Hopkins Medical Institutions as an Assistant Professor of Radiology and Acting Director of Physics and Engineering. Subsequently, he was recruited to the Department of Radiology at Columbia University and the Columbia University Medical Center of the New York-Presbyterian Hospital. Dr. Nickoloff advanced professionally to the academic title of Professor of Radiology and appointment as Chief Hospital Physicist. Dr. Nickoloff is board certified in Diagnostic Radiology Physics and Nuclear Medicine Physics by the American Board of Radiology (ABR), in Diagnostic Imaging Physics by the American Board of Medical Physics (ABMP) and in Health Physics by the American Board of Health Physics (ABHP). He has served as President of the Radiological and Medical Physics Society of New York (RAMPS, Inc.), Chairman of the American College of Medical Physics

(ACMP), Treasurer and Chair of examination panels for the ABMP, and Secretary of the Greater New York Chapter of Health Physics Society (GNYCHPS). He has served on the Board of Directors for the American Association of Physicists in Medicine (AAPM), ACMP and ABMP. Dr. Nickoloff has published 2 books, about 30 book chapters, 55 peer-reviewed journal articles, about 70 journal abstracts; his book entitled *Radiology Review: Radiologic Physics* is used by many programs training radiology residents. In addition, he has given over 130 presentations at professional meetings. He has been honored by being awarded the title of Fellow by the American College of Radiology (FACR), American College of Medical Physics (FACMP) and the American Association of Physicists in Medicine (FAAPM). He has been an active member in numerous professional organizations. Dr. Nickoloff was also honored for his lifetime achievements by the ACMP, as a recipient of the Marvin M.D. Williams Award. Dr. Nickoloff is still very active in medical physics, and he teaches Radiology residents and Applied Physics graduate students at Columbia University.